

See discussions, stats, and author profiles for this publication at: <https://www.researchgate.net/publication/7388744>

Measurement of Enzyme Activity in Single Cells by Voltammetry Using a Microcell with a Positionable Dual Electrode

ARTICLE *in* ANALYTICAL CHEMISTRY · FEBRUARY 2006

Impact Factor: 5.64 · DOI: 10.1021/ac051178c · Source: PubMed

CITATIONS

25

READS

25

4 AUTHORS, INCLUDING:



Ning Gao

Harvard University

19 PUBLICATIONS 311 CITATIONS

SEE PROFILE



Xiaoli Zhang

Shandong University

118 PUBLICATIONS 2,092 CITATIONS

SEE PROFILE

Measurement of Enzyme Activity in Single Cells by Voltammetry Using a Microcell with a Positionable Dual Electrode

Ning Gao, Minghui Zhao,[†] Xiaoli Zhang, and Wenrui Jin*

School of Chemistry and Chemical Engineering, Shandong University, Jinan 250100, China

The electrochemical single-cell analysis for enzyme activity was developed using microcells on a microcell array coupled with a positionable dual microelectrode. The microcell array with the nanoliter-scale microcells was constructed using simple chemical etching without photolithographic techniques. The positionable dual microelectrodes consisted of the nanometer-to-micrometer-radius Au disk working electrode and a $\sim 80\text{-}\mu\text{m}$ -radius Ag/AgCl reference electrode. Peroxidase was chosen as the model enzyme. Factors that concern electrochemical single-cell analysis in microcells such as solution evaporation, interference of soluble oxygen, electrode size, solution volume, and electrode fouling were investigated and discussed. The 20 or 100 nL of detection volume was found to be suitable for peroxidase determination in single neutrophils or single acute promyelocytic leukemia cells without interference from intracellular macromolecules and electrode fouling, when the dual electrode with a $10\text{-}\mu\text{m}$ -radius Au disk working electrode was used. Cells were perforated with digitonin before transferring them into the microcells, to lyse cells easily. The perforated cells were transferred into the microcells by pushing a microscope slide on a drop of the cell suspension on the microcell array. After a single cell in the microcell was lysed using a freeze–thawing technique and allowed to dry, physiological buffer saline containing 2.0×10^{-3} mol/L hydroquinone and 2.0×10^{-3} mol/L H_2O_2 as the substrates of the enzyme-catalyzed reaction was added. The microcell array was positioned in a constant-humidity chamber to prevent evaporation. Then the dual electrode was inserted into the microcell by means of a scanning electrochemical microscope and the product benzoquinone of the enzyme-catalyzed reaction was voltammetrically detected. Peroxidase activity could be quantified using the steady-state current on the voltammogram after subtracting the blank and using the calibration curve.

Single-cell analysis has been through a rapid development in the last two decades. Electrochemical detection (ECD) is a powerful tool for single-cell analysis. Voltammetry and amperometry at carbon fiber and modified carbon fiber microelectrodes have been used to measure secretion or exocytosis of neurotransmitters such

as catecholamine,^{1–5} dopamine,^{6–9} and serotonin,^{10,11} and histamine,¹⁰ and insulin^{12,13} from different kinds of cells or vesicles. Amperometric measurement of oxygen consumption at single cells using oxygen microsenors that are fabricated by coating cellulose acetate on the etched Pt wires¹⁴ has been reported. Study on the oxidative burst from fibroblasts has been performed by amperometry and voltammetry at carbon fiber platinized microelectrodes.^{15–17} Microamperometric measurement of photosynthetic activity at the single-cell level has been investigated based on detection of oxygen reduction current on the cell surface.¹⁸ A microfluidic device with microelectrodes has been used to monitor dopamine release from single cells.¹⁹ Scanning electrochemical microscopy with microelectrodes as its tip has been successfully used in single-cell analysis including investigating photosynthetic electron transport,^{18,20} detecting photosynthetic activity,^{21,22} mea-

- (1) Leszczyszyn, D. J.; Jankowski, J. A.; Viveros, O. H.; Diliberto, E. J., Jr.; Near, J. A.; Wightman, R. M. *J. Biol. Chem.* **1990**, *265*, 14736–14737.
- (2) Wightman, R. M.; Jankowski, J. A.; Kennedy, R. T.; Kawagoe, K. T.; Schroeder, T. J.; Leszczyszyn, D. J.; Near, J. A.; Diliberto, E. J., Jr.; Viveros, O. H. *Proc. Natl. Acad. Sci. U.S.A.* **1991**, *88*, 10754–10758.
- (3) Chen, T. K.; Luo, G.; Ewing, A. G. *Anal. Chem.* **1994**, *66*, 3031–3035.
- (4) Zhou, R.; Luo, G.; Ewing, A. G. *J. Neurosci.* **1994**, *14*, 2402–2407.
- (5) Xin, Q.; Wightman, R. M. *Anal. Chem.* **1998**, *70*, 1677–1681.
- (6) Garris, P. A.; Ciolkowski, E. L.; Pastore, P.; Wightman, R. M. *J. Neurosci.* **1994**, *14*, 6084–6093.
- (7) Chen, G.; Gavin, P. F.; Luo, G.; Ewing, A. G. *J. Neurosci.* **1995**, *15*, 7747–7755.
- (8) Hochstetler, S. E.; Puopolo, M.; Gustincich, S.; Raviola, E.; Wightman, R. M. *Anal. Chem.* **2000**, *72*, 489–496.
- (9) Wu, W. Z.; Huang, W. H.; Wang, W.; Wang, Z. L.; Cheng, J. K.; Xu, T.; Zhang, R. Y.; Chen, Y.; Liu, J. *J. Am. Chem. Soc.* **2005**, *127*, 8914–8915.
- (10) Pihel, K.; Hsieh, S.; Jorgenson, J. W.; Wightman, R. M. *Anal. Chem.* **1995**, *67*, 4514–4521.
- (11) Bunin, M. A.; Wightman, R. M. *J. Neurosci.* **1998**, *18*, 4854–4860.
- (12) Kennedy, R. T.; Huang, L.; Atkinson, M. A.; Dush, P. *Anal. Chem.* **1993**, *65*, 1882–1887.
- (13) Kennedy, R. T.; Huang, L.; Aspinwall, C. A. *J. Am. Chem. Soc.* **1996**, *118*, 1795–1796.
- (14) Jung, S. K.; Gorski, W.; Aspinwall, C. A.; Kauri, L. M.; Kennedy, R. T. *Anal. Chem.* **1999**, *71*, 3642–3649.
- (15) Arbault, S.; Pantano, P.; Jankowski, J. A.; Vuillaume, M.; Amatore, C. *Anal. Chem.* **1995**, *67*, 3382–3390.
- (16) Amatore, C.; Arbault, S.; Bruce, D.; de Oliveira, P.; Erard, M.; Vuillaume, M. *Faraday Discuss.* **2000**, 319–333.
- (17) Amatore, C.; Arbault, S.; Bruce, D.; de Oliveira, P.; Erard, M.; Vuillaume, M. *Chem. Eur. J.* **2001**, *7*, 4171–4179.
- (18) Yasukawa, T.; Uchida, I.; Matsue, T. *Biophys. J.* **1999**, *76*, 1129–1135.
- (19) Huang, W. H.; Cheng, W.; Zhang, Z.; Pang, D. W.; Wang, Z. L.; Cheng, J. K.; Cui, D. F. *Anal. Chem.* **2004**, *76*, 483–488.
- (20) Tsionsky, M.; Cardon, Z. G.; Bard, A. J.; Jackson, R. B. *Plant Physiol.* **1997**, *113*, 895–901.
- (21) Yasukawa, T.; Kaya, T.; Matsue, T. *Anal. Chem.* **1999**, *71*, 4637–4641.
- (22) Yasukawa, T.; Kaya, T.; Matsue, T. *Chem. Lett.* **1999**, 28, 975–976.

* Corresponding author. E-mail: jwr@sdu.edu.cn. Fax +86–531–8856–5167.

[†] Present address: Shandong Provincial Academy of Building Research.

suring respiration activity^{23–26} and redox activity,²⁷ imaging the topography,^{18,28,29} imaging the redox and acid–base reactivity,^{24,30} investigating the mechanism of charge-transfer reactions,³¹ and monitoring the neurotransmitter secretion.³² In all these studies, measurements were performed outside a single cell; i.e., the detecting microelectrode is close to an intact single cell and all detected molecules are over the cell surface. Thus, the intracellular biological molecules do not affect the measurements. Voltammetry and amperometry using microelectrodes can also be applied for concentration measurements of neurotransmitters,^{33–37} glucose,³⁸ and oxygen³⁹ in single nerve cells, as well as peroxynitrite in single myocardial cells.⁴⁰ However, since the detecting microelectrode is implanted into the cell to perform the intracellular measurement, it is surrounded by a number of high molecular weight species present in the cell cytoplasm, which might be easily adsorbed on the electrode surface and, thus, foul the electrode and cause a deterioration of the voltammetric or amperometric response of the electrode, making these in vivo experiments very difficult.³⁷ To obtain accurate results, a linear-average calibration method³⁶ or a pulse voltammetry for minimizing electrode fouling³⁷ is suggested. Recently, there has been increased interest in electrochemical detection in small volumes, as it is especially amenable to miniaturization.^{41–54} A variety of microcells are fabricated using

photolithographic and wet chemical etching techniques,^{43–46,50,54} pasting a black tape with a circular opening punched,⁴⁷ using excimer laser micromachining,⁴⁸ electrochemical etching,⁵² anisotropic etching,⁵³ and a capillary.⁵¹ In the fabricated devices, the microelectrodes are first located inside the microcells. These microcells with microelectrodes have been used to monitor purine,⁴⁵ lactate,⁵⁰ metabolic flux,⁵² catecholamine⁵³ from single cells, or transport into a single cell.⁵¹ In these electrochemical measurements, the detecting microelectrodes are in solutions, where an intact single cell is placed and the measurements are carried out outside the cell. Therefore, there is no electrode fouling from the adsorption of intracellular biological macromolecules.

In this work, we developed an electrochemical method for determination of enzyme activity inside single cells by using a nanoliter-scale microcell coupled with a positionable dual microelectrode consisted of an Au disk working electrode and an Ag/AgCl reference electrode combining enzyme-catalyzed reaction. Peroxidase (PO), a heme protein, was chosen as the model enzyme. In this method, the microcell arrays were simply constructed using chemical etching without photolithographic techniques. The positionable dual electrodes were fabricated by integrating a working microelectrode and a reference microelectrode into a thick-septum borosilicate twin tubing (θ tubing). The solution evaporation, interference of soluble oxygen in the detected solution, electrode size, solution volume, electrode fouling, as well as single cell sampling, transferring into the microcell, and cytolysis were investigated and discussed. The method was applied to determine PO activity in single neutrophils and single acute promyelocytic leukemia (APL) cells.

EXPERIMENTAL SECTION

Chemicals. 2-Allylphenol (99%) was purchased from Acros Organics (Geel, Belgium). The 4.5% dextran T-500 was prepared by dissolving appropriate dextran T-500 (Pharmacia Co., Uppsala, Sweden) in 1 mL of physiological buffer saline (PBS). Lymphocyte separation medium was purchased from Shanghai Hengxin Chemical Reagents Co. Ltd. (Shanghai, China). Horseradish peroxidase (HRP, R.Z. \sim 3.0, 250 units/mg) was obtained from Shanghai Lizhu Dongfeng Biotechnology Co. Ltd. (Shanghai, China). PBS consisted of 0.15 mol/L NaCl, 7.6×10^{-3} mol/L Na_2HPO_4 , and 2.4×10^{-3} mol/L NaH_2PO_4 (pH 7.4). All aqueous solutions were prepared with doubly distilled water. Etching solution contained 60% (by volume) saturated CaCl_2 , 4% HCl, and 36% doubly distilled water. Coating solution was prepared by dissolving 0.0283 g of phenol, 0.0616 g of 2-allylphenol and 0.0888 g of ethylene glycol monobutyl ether in 5 mL of a 1:1 methanol/water mixture. For nanometer-sized electrodes, the coating solution was directly used. For micrometer-sized electrodes, the coating solution was used after adjusting the pH to 9.0 with ammonia/water. Hydroquinone (analytical grade), benzoquinone (chemical grade), H_2O_2 (content \geq 30%, analytical grade), digitonin,

- (23) Yasukawa, T.; Kondo, Y.; Uchida, I.; Matsue, T. *Chem. Lett.* **1998**, 27, 767–768.
- (24) Liu, B.; Cheng, W.; Rotenberg, S. A.; Mirkin, M. V. *J. Electroanal. Chem.* **2001**, 500, 590–597.
- (25) Shiku, H.; Shiraishi, T.; Ohya, H.; Matsue, T.; Abe, H.; Hoshi, H.; Kobayashi, M. *Anal. Chem.* **2001**, 73, 3751–3758.
- (26) Kaya, T.; Torisawa, Y. S.; Oyamatsu, D.; Nishizawa, M.; Matsue, T. *Biosens. Bioelectron.* **2003**, 18, 1379–1383.
- (27) Liu, B.; Rotenberg, S. A.; Mirkin, M. V. *Proc. Natl. Acad. Sci. U.S.A.* **2000**, 97, 9855–9860.
- (28) Feng, W.; Rotenberg, S. A.; Mirkin, M. V. *Anal. Chem.* **2003**, 75, 4148–4154.
- (29) Liebetrau, J. M.; Miller, H. M.; Baur, J. E.; Takacs, S. A.; Anupunpisit, V.; Garriss, P. A.; Wipf, D. O. *Anal. Chem.* **2003**, 75, 563–571.
- (30) Cai, C.; Liu, B.; Mirkin, M. V.; Frank, H. A.; Rusling, J. F. *Anal. Chem.* **2002**, 74, 114–119.
- (31) Liu, B.; Rotenberg, S. A.; Mirkin, M. V. *Anal. Chem.* **2002**, 74, 6340–6348.
- (32) Hengstenberg, A.; Blöchl, A.; Dietzel, I. D.; Schuhmann, W. *Angew. Chem., Int. Ed.* **2001**, 40, 905–908.
- (33) Meulemans, A.; Poulain, B.; Baux, G.; Tauc, L.; Henzel, D. *Anal. Chem.* **1986**, 58, 2088–2091.
- (34) Meulemans, A.; Poulain, B.; Baux, G.; Tauc, L. *Brain Res.* **1987**, 414, 158–162.
- (35) Chien, J. B.; Wallingford, R. A.; Ewing, A. G. *J. Neurochem.* **1990**, 54, 633–638.
- (36) Lau, Y. Y.; Chien, J. B.; Wong, D. K. Y.; Ewing, A. G. *Electroanalysis* **1991**, 3, 87–95.
- (37) Chen, T. K.; Lau, Y. Y.; Wong, D. K. Y.; Ewing, A. G. *Anal. Chem.* **1992**, 64, 1264–1268.
- (38) Abe, T.; Lau, Y. Y.; Ewing, A. G. *J. Am. Chem. Soc.* **1991**, 113, 7421–7423.
- (39) Lau, Y. Y.; Abe, T.; Ewing, A. G. *Anal. Chem.* **1992**, 64, 1702–1705.
- (40) Xue, J.; Ying, X.; Chen, J.; Xian, Y.; Jin, L. *Anal. Chem.* **2000**, 72, 5313–5321.
- (41) Bowyer, W. J.; Clark, M. E.; Ingram, J. L. *Anal. Chem.* **1992**, 64, 459–462.
- (42) Pantano, P.; Kuhr, W. G. *Electroanalysis* **1995**, 7, 405–416.
- (43) Bratten, C. D. T.; Cobbold, P. H.; Cooper, J. M. *Anal. Chem.* **1997**, 69, 253–258.
- (44) Clark, R. A.; Hietpas, P. B.; Ewing, A. G. *Anal. Chem.* **1997**, 69, 259–263.
- (45) Bratten, C. D.; Cobbold, P. H.; Cooper, J. M. *Anal. Chem.* **1998**, 70, 1164–1170.
- (46) Clark, R. A.; Ewing, A. G. *Anal. Chem.* **1998**, 70, 1119–1125.
- (47) Nagy, G.; Xu, C. X.; Buck, R. P.; Lindner, E.; Neuman, M. R. *Anal. Chem.* **1998**, 70, 2156–2162.
- (48) Ball, J. C.; Scott, D. L.; Lumpkin, J. K.; Daunert, S.; Wang, J.; Bachas, L. G. *Anal. Chem.* **2000**, 72, 497–501.
- (49) Spaine, T. W.; Baur, J. E. *Anal. Chem.* **2001**, 73, 930–938.

- (50) Cai, X.; Klauke, N.; Glidle, A.; Cobbold, P.; Smith, G. L.; Cooper, J. M. *Anal. Chem.* **2002**, 74, 908–914.
- (51) Troyer, K. P.; Wightman, R. M. *Anal. Chem.* **2002**, 74, 5370–5375.
- (52) Yasukawa, T.; Glidle, A.; Cooper, J. M.; Matsue, T. *Anal. Chem.* **2002**, 74, 5001–5008.
- (53) Chen, P.; Xu, B.; Tokranova, N.; Feng, X.; Castracane, J.; Gillis, K. D. *Anal. Chem.* **2003**, 75, 518–524.
- (54) Neugebauer, S.; Evans, S. R.; Aguilar, Z. P.; Mosbach, M.; Fritsch, I.; Schuhmann, W. *Anal. Chem.* **2004**, 76, 458–463.

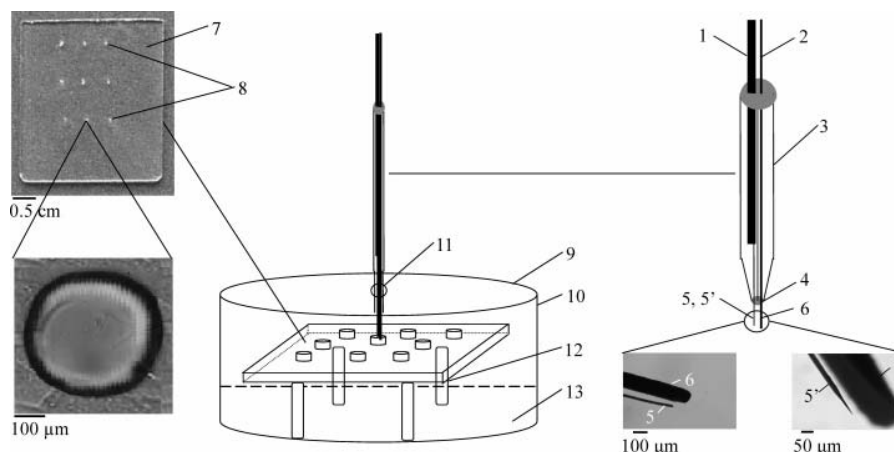


Figure 1. Schematic diagram of the setup with microcell array and dual electrode in a constant-humidity chamber for single-cell analysis: 1, copper lead; 2, Ag wire; 3, dual electrode; 4, epoxy resin; 5, micrometer-sized Au disk working electrode; 5', nanometer-sized Au disk working electrode; 6, Ag/AgCl reference electrode; 7, wax; 8, microcell array; 9, cover; 10, Petri dish as a constant-humidity chamber; 11, hole; 12, stand; 13, water.

and other chemicals (analytical grade) were purchased from standard reagent suppliers. Several steps described in our previous work⁵⁵ were taken to minimize contamination.

Apparatus. A CHI 800 electrochemical analyzer (CH Instruments, Austin, TX) was used to perform electrode characterization and voltammetric measurements of PO activity in the HRP standard solution and cell extracts after the enzyme-catalyzed reaction. A CHI 900 scanning electrochemical microscope (CH Instruments) was employed to accomplish approach curves and voltammetric measurements of PO activity in single cells after the enzyme-catalyzed reaction.

Fabrication of Dual Electrodes with a Micrometer- or Nanometer-Sized Au Disk Working Electrode and a Micrometer-Sized Ag/AgCl Reference Electrode. First, micrometer- or nanometer-sized Au disk working electrodes and micrometer-sized Ag/AgCl reference electrodes were constructed, respectively. The micrometer-sized Au electrodes were constructed using 10- μ m-radius, \sim 1.5-cm-long Au wires (Heraeus Zhaoyuan Precious Metal Materials Co., Ltd., Zhaoyuan, China). One end of the Au wire was glued to a 150- μ m-radius, \sim 8-cm-long copper lead with silver epoxy. The ensemble was cured for 30 min at 150 $^{\circ}$ C in an oven. Epoxy resin was then applied to the junction between the Au wire and the copper lead in order to isolate and protect the electrical junction. After 24 h, the exposed Au wire was electrochemically coated with extremely thin insulation film. The procedure was similar to the method reported by Strein and Ewing.⁵⁶ The tip of the Au wire was dipped in the pH 9.0 coating solution for electropolymerization. A dc voltage of 4 V was applied between the Au wire and a 250- μ m-radius, \sim 6-mm-long Pt wire for 20 min. The Au wire was removed from the solution and cured by placing it in an oven at 150 $^{\circ}$ C for 30 min, to induce film shrinkage and expose the surface at the apex. To fabricate nanometer-sized electrodes, the apex of the 10- μ m Au wire of the ensemble was electrochemically etched to an ultrafine point. The procedure was similar to the method reported by Sun et al.⁵⁷ A 100- μ m-radius Pt ring was covered with a film of the

etching solution. After the Au wire was inserted into the etching solution by means of a laboratory-made xyz micromanipulator, a 50-Hz ac voltage of 20 V was applied between the Au wire and the Pt ring using an ultralow frequency signal generator (XD5A, Tianjin Instrument Co., Tianjin, China). The bubbles were formed at the Au/solution interface and could be observed during electrochemical etching. The applied voltage was removed immediately upon cessation of bubbling, and the Au wire was taken out from the etching solution. The Au wire was cleaned by doubly distilled water for 5 min in an ultrasonicator. After drying, the tip of the Au wire was dipped in the coating solution for electropolymerization. A dc voltage of 4 V was applied between the etched Au wire and a 250- μ m-radius, \sim 6-mm-long Pt wire for 4 min. The electrode was removed from the solution and cured by placing it in an oven at 150 $^{\circ}$ C for 30 min. While curing, the polymer retracted from the sharpened tip of the wire, exposing the electrode surface at the apex. The micrometer-sized Ag/AgCl reference electrode was constructed by electrodepositing in 1 mmol/L KCl using a 60- μ m-radius, \sim 8-cm-long Ag wire. The Au–Ag/AgCl dual electrodes were constructed using borosilicate θ tubing (BT-150-10, Sutter Instrument Co. Novato, CA), named for its resemblance to the Greek letter theta (θ). The borosilicate θ tubing was pulled using a P-2000 laser micropipet puller (Sutter Instrument Co.) to make a dual pipet with two orifices (\sim 100- μ m o.d.). Then, a micrometer- or nanometer-sized Au disk working electrode and a micrometer-sized Ag/AgCl reference electrode were inserted into two sides of the thick-septum borosilicate θ tubing, respectively. Both electrodes were secured in the θ tubing and the top of the θ tubing was sealed with insulating epoxy resin. The reference electrode was protruded \sim 2 mm from the top of the θ tubing and slightly longer than the working electrode. The working electrode and the reference electrode of the dual electrodes were almost parallel (Figure 1).

Fabrication of Microcells. The microcell array was shown in Figure 1. A thin wax layer of \sim 2-mm thickness with holes that were punched manually using a sewing needle with a 50- μ m-diameter tip was constructed on a microscope glass slide. The glass slide was etched by dropping 40% HF into the holes. During etching, the HF solution was changed every 2 h. (*Caution:* 40%

(55) Sun, X.; Jin, W. *Anal. Chem.* **2003**, *75*, 6050–6055.

(56) Strein, T. G.; Ewing, A. G. *Anal. Chem.* **1992**, *64*, 1368–1373.

(57) Sun, P.; Zhang, Z.; Guo, J.; Shao, Y. *Anal. Chem.* **2001**, *73*, 5346–5351.

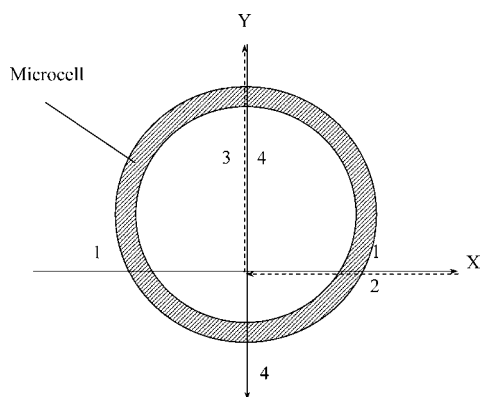


Figure 2. Process of finding the tip position above a microcell by using SECM scan curve (current versus tip position curve).

HF can cause severe lesions! Care should be taken to avoid skin contact.) Then HF was removed by washing with tap water. After warming the slide using an electric fan, the wax on the slide was removed with a knife. The rest wax power was removed by rinsing with tap water, *n*-hexane, tap water, and doubly distilled water, respectively. The microcells with 200–710- μm diameter at the top and 150–620- μm diameter at the bottom could be constructed by controlling the hole diameter and the etching time. The depth of the microcells was measured by scanning electrochemical microscope (SECM) using the recording of two approach curves. First, the slide with microcells was placed in a Petri dish as the electrochemical cell with a Pt counter electrode and an Ag/AgCl reference electrode. Then 1.00×10^{-2} mol/L $\text{K}_3\text{Fe}(\text{CN})_6$ and 0.5 mol/L KCl were added over the slide. A 10- μm -radius Au tip was positioned above the slide. The Au tip potential was held at 0 V versus Ag/AgCl. The tip was moved slowly and vertically down to the slide, and the curve of the tip current (i) versus the displacement was recorded. The tip current decreased with the distance due to negative feedback as the tip was close to the slide. When i was 80% of the steady-state current, the tip was stopped. In this case, the distance between the tip and the slide surface could be estimated using the fit of the experimental normalized approach curve to theory based on the method reported by Bard et al.⁵⁸ From this fitting, the distance was estimated to be ~ 20 μm . Then, the tip was moved laterally toward the microcell at a constant height according to the traces shown in Figure 2, to search the microcell center. When the tip was moved along the x -axis above a microcell (solid line 1), i increased, because the effect of the negative feedback was reduced. When i decreased, implying that the tip left the microcell, the tip was moved back (dashed line 2) and stopped at the position of maximum current. Then, the tip was moved along the y -axis (dashed line 3) and crossed the whole microcell, which could be observed as i was reduced. Finally, the tip was scanned reversely along the same trace (solid line 4) and stopped at the position of the maximum current, meaning the position of the microcell center. The tip was moved slowly and vertically down to the bottom of the microcell to record the second approach curve. When i was 80% of the steady-state current, the tip was stopped. In this case, the distance between the tip and the microcell bottom was ~ 20 μm . Thus, one

could obtain the depth of the microcell from the traveling distance of the tip during performance of the second approach curve. Using this method, measured microcell depth was between 100 and 320 μm . The volumes of the microcells were calculated to be between 2 and 112 nL. In single-cell analysis, ~ 25 nL for neutrophils and ~ 110 nL for APL cells were used.

Preparation of Cells and Their Extract. Human neutrophils were isolated as described previously.⁵⁹ Briefly, five portions of human blood and one portion of 4.5% dextran T-500 separation solution were mixed in a 10-mL centrifuge tube. The mixture was allowed to stand for 40 min at 4 $^{\circ}\text{C}$. The light red transparent supernatant liquid contained neutrophils, a few lymphocytes, and erythrocytes. Three portions of the supernatant liquid were put on one portion of lymphocyte separation medium and then were centrifuged for 15 min at 1000 rpm. The supernatant and the middle foggy layer containing lymphocytes were discarded. The cell mixtures at the bottom contained neutrophils and a small amount of erythrocytes. Following washing with 2 mL of PBS buffer, the cell mixture was centrifuged for 3 min at 2000 rpm. The supernatant was discarded. Then 2 mL of H_2O was added. After vibrating the solution for ~ 20 s, erythrocytes were lysed. Two milliliters of 1.8% NaCl was immediately added into the cell mixture, and the mixture was centrifuged for 3 min at 2000 rpm. The supernatant was discarded again. Following two washing steps ~ 10 μL of neutrophil solution could be obtained. Then 1 mL of PBS buffer was added to the neutrophil solution to obtain the neutrophil suspension. To lyse cells easily, chemical perforation of the cell membrane was accomplished. A 1.0×10^{-4} mol/L solution of digitonin was added to the neutrophil suspension with a final concentration of 5.0×10^{-6} mol/L. Fifteen minutes later, the digitonin was removed by washing with PBS and centrifugating. After addition of 1 mL of PBS, the cell suspension was counted using a hemocytometer (Shanghai Medical Optical Instrument Plant, Shanghai, China) under an inverted biological microscope. The perforated neutrophils were immediately used to determine enzyme activity in single cells. To prepare the cell extract, a part of the perforated neutrophil suspension was ultrasonicated and stored at 4 $^{\circ}\text{C}$.

Acute promyelocytic leukemia cells were provided by the Department of Hematology, Qilu Hospital of Shandong University (Jinan, China). The procedure of preparation of the cell extract was the same as that for neutrophils.

Determination of HRP Activity in the Standard Solution and PO Activity in the Cell Extract. The activity of all peroxidases is defined and determined with the same method. Therefore, HRP served as a standard to quantify PO activity and the same activity unit for both HRP and PO was used in this work. Detection of both HRP activity in the standard solution and PO activity in the cell extract was carried out in a 5- μL electrochemical cell containing PBS, 2.0×10^{-3} mol/L H_2Q , and 2.0×10^{-3} mol/L H_2O_2 by voltammetry at a dual electrode with a 10- μm -radius Au disk working electrode. After the HRP standard solution or cell extract was added in the electrochemical cell, the voltammogram was recorded immediately from 0.05 to -0.4 V as the blank. Then, the solution was incubated for 10 min and the voltammogram was recorded. After subtracting the blank, the steady-state current was used for quantification using the standard calibration method.

(58) Bard, A. J.; Fan, F. R. F.; Kwak, J.; Lev, O. *Anal. Chem.* **1989**, *61*, 132–138.

(59) Jin, W.; Jiang, L. *Electrophoresis* **2002**, *23*, 2471–2476.

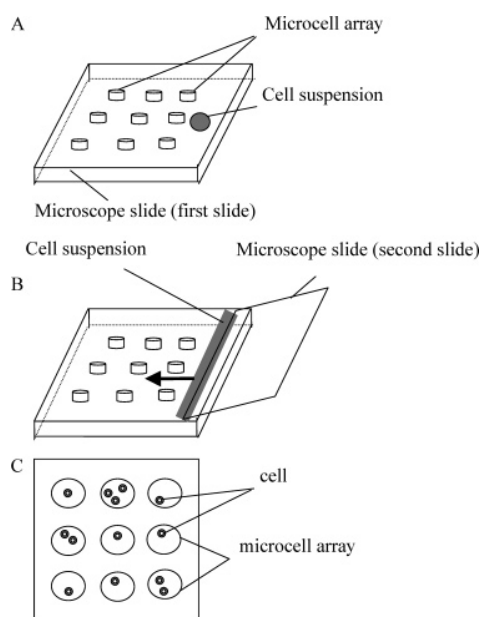


Figure 3. Schematic diagram of introducing cells into the microcells.

Single-Cell Analysis. To introduce single cells into microcells, a simple and rapid method by pushing a microscope slide on the microcell array was adopted. The cell introduction process is shown in Figure 3. The cell suspension was diluted to $\sim 10^4$ cell/mL with PBS. A drop of the diluted cell suspension was deposited onto the side of the slide (the first slide) with the microcell array (Figure 3A). Another microscope slide (the second slide) was held by the tips of the index finger and the thumb and its placed edge on the drop of the cell suspension at a $\sim 30^\circ$ angle (Figure 3B). The cell suspension was distributed along the edge of the second slide. Then, the second slide was pushed along the surface of the first slide to introduce cells into the microcells. In this case, one or more than one cell could be delivered into the individual microcells (Figure 3C). The microcells with one cell were selected under an inverted biological microscope with a magnification of $400\times$ and used for single-cell analysis. The microcell array with cells was positioned on the stand of a Petri dish (5 cm in diameter and 0.8 cm in height). The cells were subjected to freeze–thawing for cytolysis. The Petri dish was maintained for 30 min at -20°C in a refrigerator. Then, the Petri dish was taken out and kept at room temperature for defrosting. This process was repeated three or four times to lyse the cells and obtain the single-cell extract containing intracellular substances involving PO. In the experiments, ~ 25 nL of microcells for neutrophils and ~ 110 nL of microcells for APL cells were used. The extracts in the microcells were allowed to evaporate for ~ 2 min for neutrophils and for ~ 5 min for APL cells. Then, 20 (for neutrophils) or 100 nL (for APL cells) of PBS containing 2.0×10^{-3} mol/L H_2Q and 2.0×10^{-3} mol/L H_2O_2 was added using a laboratory-made microinjector fabricated from a $25\text{-}\mu\text{m}$ -i.d., 4.1-cm-long capillary with a relative standard deviation of 2.4% and a $50\text{-}\mu\text{m}$ -i.d., 5.1-cm-long capillary with a relative standard deviation of 2.1% to redissolve the intracellular substances. The microcell array was positioned on the stand of the Petri dish again. Water was added under the stand of the Petri dish as a constant-humidity chamber, and the cover with an access hole was put on (see Figure 1) to prevent evaporation. Then, the dual electrode held on the electrode stand

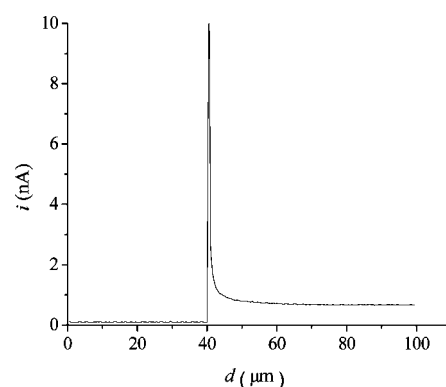


Figure 4. Electrochemical approach curves of the tip from air to solution in a microcell.

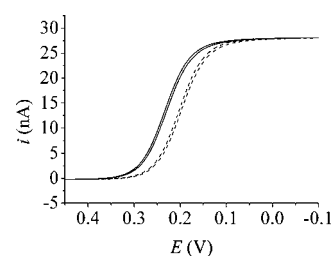


Figure 5. Cyclic voltammograms using a two-electrode system consisting of a $10\text{-}\mu\text{m}$ -radius dual electrode (dashed line) and a three-electrode system consisting of the same working electrode, a normal Ag/AgCl reference electrode, and a Pt counter electrode (solid line). 0.5 mol/L KCl containing 1.00×10^{-2} mol/L $\text{K}_3\text{Fe}(\text{CN})_6$; scan rate, 50 mV/s.

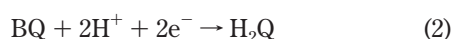
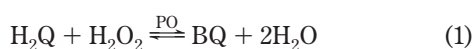
of SECM with a potential of 0.7 V for the Au disk working electrode was inserted into a microcell through the access hole by means of SECM according to the following steps. The dual electrode was moved from air into the solution. When the dual electrode entered the solution, the current sharply rose, then attained the steady-state current, and maintained a constant value because of the oxidization of H_2Q at the Au disk working electrode as more of the dual electrode immersed into the solution. The air/solution approach curve (current (i) versus displacement (d)) is shown in Figure 4. Then the electrode was slowly moved down toward the bottom of the microcell. Using the method, the depth of the dual electrode in the solution was controlled at $\sim 100\text{ }\mu\text{m}$. Then, the voltammogram was recorded from 0.05 to -0.4 V as the blank. Finally, the solution was incubated for 10 min and the voltammogram was recorded again. After subtracting the blank, the steady-state current was used for quantification using the standard calibration method.

RESULTS AND DISCUSSION

Detection of HRP Activity in the Standard Solution and PO Activity in the Cell Extract. Before detecting the enzyme activity, the characteristics of the dual electrode were investigated. Figure 5 compares voltammograms of 1.00×10^{-2} mol/L $\text{K}_3\text{Fe}(\text{CN})_6$ in 0.5 mol/L KCl recorded using a two-electrode system that consists of a dual electrode with a $10\text{-}\mu\text{m}$ -radius Au disk working electrode and a three-electrode system consisting of the same Au disk working electrode (the reference electrode in the dual electrode was not used in this case), a normal Ag/

AgCl reference electrode, and a Pt counter electrode. The most notable difference between the two voltammograms was the negative shift in half-wave potential, when the dual electrode was used. To explore the reason for this shift, the voltammogram was recorded using a three-electrode system consisting of the dual electrode and a Pt counter electrode. Almost the same shift was observed. This means that this shift arose from the shielding effect of the reference electrode of the dual electrode rather than from no iR drop compensation, when the two-electrode system was used. It is clear from the identical shape and steady-state current of the voltammograms that the negative shift in half-wave potential was not an important factor for determination of steady-state current as the dual electrode was used. The sigmoidal cyclic voltammograms were also obtained for the dual electrodes with the Au disk working electrodes of 500-, 120-, and 23-nm radii.

PO can convert enzyme substrates H_2Q into its product benzoquinone (BQ) according to reaction 1 in the presence of



H_2O_2 at a relatively high reaction rate. As the result of enzyme amplification, a significant amount of product, which provides amplification of signal, can be produced for final voltammetric detection at the working electrode according to eq 2.

Since both PO and HRP are the peroxidase, both of them can catalyze the same substrates with the same mechanism. Therefore, HRP could be used to investigate the optimal conditions for detection of PO activity. For detection of HRP activity through the enzyme-catalyzed reaction, the standard HRP was used to react with its substrates (H_2Q and H_2O_2). It was found that 2.0×10^{-3} mol/L H_2Q , 2.0×10^{-3} mol/L H_2O_2 in PBS (pH 7.4), and the reaction time of 10 min were suitable for the detection of HRP. To explore whether the soluble oxygen interfered with the determination of HRP activity or PO activity, the voltammogram in PBS was recorded using the dual electrode with a $10\text{-}\mu\text{m}$ -radius Au disk working electrode as shown in Figure 6, curve 1. The voltammogram clearly shows that the obvious current of oxygen reduction appeared on the voltammogram. Therefore, the current of oxygen reduction should be subtracted for measurement of the reduction current of product BQ of the enzyme-catalyzed reaction. In following experiments, the voltammograms corresponding to oxygen reduction as the blank were recorded and all voltammograms after subtracting the blank were recorded. In Figure 6, curves 2 and 3 show the voltammograms in the presence of 8.3×10^{-4} mol/L HRP before and after subtracting the current of oxygen reduction. The steady-state current after subtracting the current of oxygen reduction could be used to quantify HRP activity (i.e., PO activity). The linear range of HRP activity concentration (i.e., PO activity concentration) was 8.00×10^{-5} – 3.30×10^{-3} unit/mL with a correlation coefficient of 0.996. The relative standard deviation (RSD) for an activity concentration of 8.0×10^{-4} unit/mL HRP was 1.9% ($n = 10$).

Since the detected potential ranged from 0.05 to -0.4 V, the electroactive compounds such as cysteine, histidine, tryptophan, tyrosine, dopa, dopamine, serotonin, epinephrine, and norepinephrine, which can be directly oxidized at the working

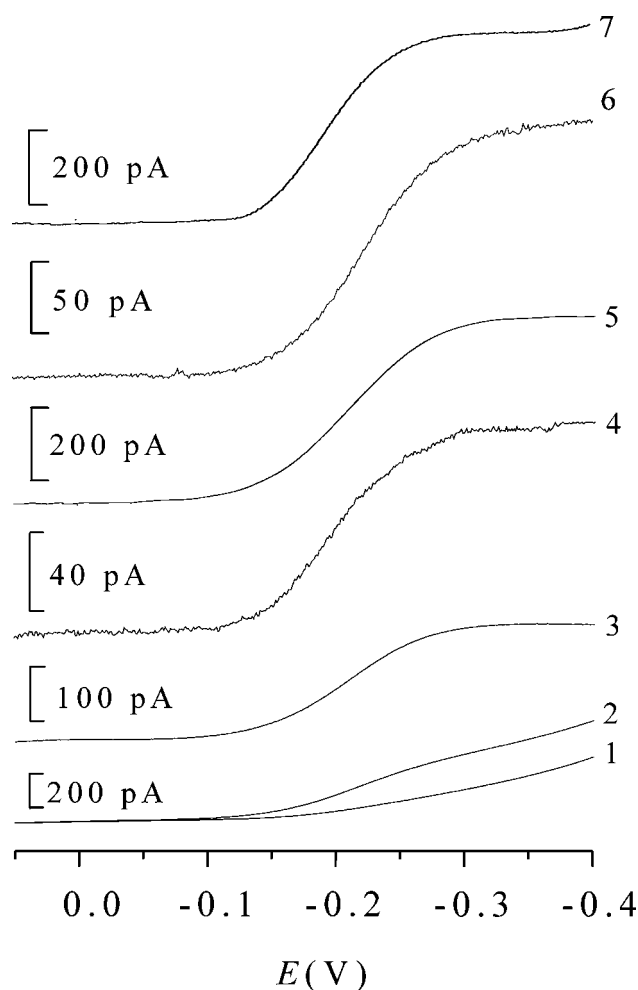


Figure 6. Linear scan voltammograms of (1) 2.0×10^{-3} mol/L H_2Q , 2.0×10^{-3} mol/L H_2O_2 in PBS (pH 7.4); (2) (1) + 8.3×10^{-4} unit/mL HRP after incubation for 10 min; (3) (2) after subtracting curve 1; (4) (1) + the neutrophil extract corresponding to a neutrophil in 20 nL; (5) (1) + the APL cell extract corresponding to 0.97 APL cell in 100 nL; (6) a single lysed neutrophil; (7) a single lysed APL cell. (4–7) After incubation for 10 min and after subtracting blank. Dual electrode and scan rate as in Figure 5.

electrode, did not interfere with the determination of PO activity. To know whether the biological macromolecules in cells foul the Au working electrode, 40 voltammograms were continuously recorded using a dual electrode in the neutrophil extract corresponding to 1.2 cells in 20 nL and shown in Figure 7A. The steady-state current with multiple scanning due to the enzyme-catalyzed reaction. The same phenomenon was observed for the standard HRP solution (Figure 7B). This indicates that the reproducibility of the dual electrode in the cell extract is fine and the working electrode was not fouled. In Figure 6, curve 4 shows a typical voltammogram of the neutrophil extract corresponding to a neutrophil in 20 nL after subtracting the blank. Ten neutrophil extracts were determined, and the data were listed in Supporting Information. To prove the reliability of the method, a certain amount of standard HRP was added to the extracts and then the extracts were measured. From the detected activity concentrations in the neutrophil extracts with and without the standard HRP, the recoveries calculated are between 96 and 106%. According to the activity concentrations determined and the cell concentrations

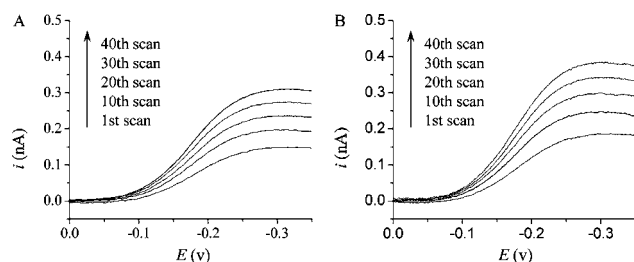


Figure 7. Multiple linear scan voltammograms (A) in the neutrophil extract corresponding to 1.2 neutrophils in 20 nL and (B) in 6.5×10^{-4} unit/mL HRP solution after incubation for 10 min and subtracting blank. Dual electrode and scan rate as in Figure 5.

for the 10 neutrophil extracts, the calculated mean PO activity in a single neutrophil was $(1.3 \pm 0.42) \times 10^{-8}$ unit (mean \pm standard deviation), which was within the range of values $(0.11\text{--}6.4) \times 10^{-8}$ unit) determined in single-cell analysis by using microfluidic chip-ECD and high-throughput ECD in a capillary as a sampler and reactor (will be reported elsewhere). Among all subtypes of leukemia, APL cells have the highest PO activity.^{60,61} A typical voltammogram of the APL cell extract corresponding to 0.97 APL cell in 100 nL after subtracting the blank is shown in Figure 6, curve 5. Ten APL cell extracts were determined, and the data were listed in Supporting Information. According to the determined activity concentrations and the cell concentrations for the 10 APL cell extracts, the calculated mean PO activity in a single APL cell was $(2.3 \pm 0.54) \times 10^{-7}$ unit. PO activity in APL cells was ~ 10 times higher than that in neutrophils.

Single-Cell Analysis Using a Microcell Coupled with a Dual Electrode. Solution evaporation must be considered when measurements are performed with microcells except for on-chip microfluidics, in which evaporation is minimized or eliminated with the covered system.⁶² Several methods such as mixing a liquid having a high vapor pressure,^{44,46,48} placing a sample under a protective layer of an immiscible fluid,^{43,45,50,52,53,63–65} and using a solvent-saturated environment^{41,44,49} are often used to prevent or minimize evaporation. A fast-scan voltammetry with a scan rate of 50 V/s can also be used in the microcell without protection from evaporation, because the measurement is finished before solution evaporation.⁵⁴ To prevent quick evaporation of solution in microcells in our work, single-cell analysis experiments were carried out in a constant-humidity chamber shown in Figure 1, where the microcell array was positioned. To know whether the solution is evaporated over the course of an experiment with a 20-nL microcell, the voltammograms were recorded in 1.00×10^{-2} mol/L $\text{K}_3\text{Fe}(\text{CN})_6$ in 0.5 mol/L KCl at different times. Almost the same voltammograms were obtained within 15 min, meaning that the chamber maintained a water vapor-saturated atmosphere and there were no significant changes in concentration in the microcell due to evaporation during determination of PO activity in a single cell (<13 min).

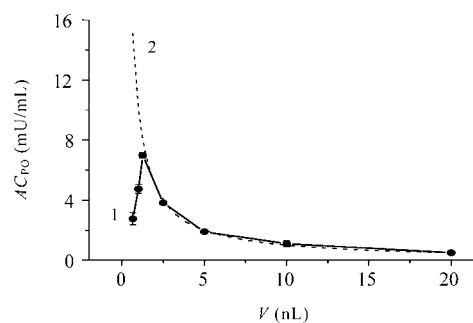


Figure 8. Dependences of the PO activity concentration, AC_{PO} , (1) detected (solid line) and (2) expected (dashed line) in different neutrophil extracts on the solution volume occupied by one neutrophil, V . The expected AC_{PO} were calculated from the detected PO value in the neutrophil extract, where a neutrophil occupied 20 nL. Conditions as in Figure 6(4).

To select electrode size, the disk working electrodes with radii of 23 nm, 500 nm, and 10 μm were attempted for single-cell analysis. For a 23-nm-radius Au electrode, the steady-state current was too low for determination of PO activity in a single cell. When a 500-nm-radius Au electrode was used, PO activity in a single cell could be determined, but the incubation time had to be longer than 30 min. When a 10- μm disk working electrode was used, a sufficient S/N for determination of PO activity in single cells could be obtained for incubation of 10 min. Therefore, 10- μm disk working electrodes were used in our experiments. The voltammogram of a 10- μm electrode in the extract corresponding to a neutrophil in 20 nL after incubation for 10 min is shown in Figure 6, curve 4.

Additionally, when electrochemical single-cell analysis is carried out in a microcell, two factors must be considered. First, the solution volume should be small enough so that the concentration of the analyte of interest in the detected solution can be detected. Second, the solution volume should be large enough; in other words, the concentrations of other biological macromolecules from a single cell should be low enough so that these macromolecules do not interfere with the determination of the analyte of interest. To determine the suitable solution volume for PO activity measurement in single-cell analysis, linear scan voltammograms of the neutrophil extracts with different concentrations corresponding to different solution volumes occupied by one cell were recorded. The PO activity concentrations, AC_{PO} , were obtained from the steady-state currents after subtracting the blank using the standard calibration method. The relationship between AC_{PO} and the solution volume occupied by one cell, V , is shown in Figure 8, curve 1. For comparison, the expected relationship between AC_{PO} and V , which was calculated from the detected PO activity concentration in the extract, where one cell occupied 20 nL, is shown in Figure 8, curve 2. By comparing curves 1 and 2, it was found that when $V \leq 2.5$ nL, detected AC_{PO} departed from the expected values. The possible reasons were the interference from biological macromolecules, the electrode fouling, or both. To verify the conclusion, the recovery experiments were done for the neutrophil extracts with different concentrations corresponding to different solution volumes occupied by one cell. In the recovery experiments, a certain amount of HRP standard was added to each extract with the activity concentration, C_{extract} , that was determined previously. The activity concentration of the

(60) Reynolds, W. F.; Chang, E.; Douer, D.; Ball, E. D.; Kanda, V. *Blood* **1997**, 90, 2730–2737.

(61) Klobusicka, M.; Kusenda, J. D.; Babusikova, O. *Neoplasma* **2005**, 52, 211–218.

(62) Figeys, D.; Pinto, D. *Anal. Chem.* **2000**, 72, 330A–335A.

(63) Yi, C.; Gratzl, M. *Anal. Chem.* **1994**, 66, 1976–1982.

(64) Yi, C.; Huang, D.; Gratzl, M. *Anal. Chem.* **1996**, 68, 1580–1584.

(65) Kashyap, R.; Gratzl, M. *Anal. Chem.* **1998**, 70, 1468–1476.

Table 1. Recoveries of Determination of PO Activity Concentration in Neutrophil Extracts, Where One Cell Occupies Different Solution Volumes

soln vol of one cell (nL)	PO activ concn (mU/mL)	PO activ concn added (mU/mL)	PO activ concn detected (mU/mL)	recovery
20	0.505	0.500	1.01, 1.02, 1.00	101, 103, 99
10	1.00	1.00	2.29, 2.32, 2.26	101, 104, 98
5	1.90	2.00	3.82, 3.80, 3.92	96, 95, 101
2.5	3.83	4.00	7.22, 7.19, 7.31	85, 84, 87
1.25	6.96	8.00	12.6, 12.4, 13.1	70, 68, 76

extract after adding the HRP standard was determined to be C_{found} . From C_{extract} , C_{found} , and the activity concentration of HRP in the extract, C_{add} , the recovery could be calculated by the following equation:

$$\text{recovery (\%)} = [(C_{\text{found}} - C_{\text{extract}})/C_{\text{add}}] \times 100 \quad (3)$$

The recoveries for five neutrophil extracts are listed in Table 1. It is seen that only when $V \geq 5$ nL were the recoveries close to 100%. The results are in agreement with that obtained shown in Figure 8, implying that ≥ 5 -nL solution volume could be used to determine PO in single neutrophils without interference from intracellular macromolecules. Based on the PO activity in single cells, 20 (for neutrophils) or 100 nL (for APL cells) of solution volume was used in the single-cell analysis experiments.

Single-cell sampling and transferring a single cell into a microcell are two important steps for single-cell analysis. Usually, the microinjector with a micropipet^{45,50–52} is used by means of a microscope. We developed a simple method to transfer single cells into the microcells on the microcell array by pushing a microscope slide on a drop of the cell suspension. The detail of the procedure was described in Experimental Section. Cytolysis was accomplished using the freeze–thaw technique. To lyse easily, the neutrophils were chemically perforated with digitonin that bound to cholesterol on the cell membrane and micropores were formed before freeze. After cytolysis, the solution was allowed to stand for ~ 2 min for neutrophils or for ~ 5 min for APL cells until the solution was evaporated. Then, 20 (for single-neutrophil analysis) or 100 nL (for single-APL cell analysis) of PBS containing 2.0×10^{-3} mol/L H_2Q and 2.0×10^{-3} mol/L H_2O_2 was added into the microcell to redissolve PO from the cell. Inserting the dual electrode into the microcell was also difficult, because the dual electrode was broken easily. To overcome the difficulty, we used SECM to insert the dual electrode according to the procedure described in the Experimental Section. After the dual electrode was inserted into the microcell, the linear scan voltammogram as blank was recorded. In this case, both oxygen reduction current and BQ reduction current during inserting the dual electrode into the microcell were responsible for the blank. Then, the solution was incubated for 10 min and the linear scan voltammogram was recorded again. Since the steady-state current was proportional to the incubation time during determination of PO activity including inserting the dual electrode into the microcell, incubating the solution, and recording the voltammogram, the small time difference for inserting the dual electrode into the microcell between detecting standard solutions and single-cell extracts did

not affect the determination of PO activity. A typical voltammogram of a single neutrophil after subtracting the blank is shown in Figure 6, curve 6. The PO activity in 18 individual neutrophils was determined (see Supporting Information). The PO activities were in the range from 0.65 to 2.1×10^{-8} unit with a mean PO activity of $(1.2 \pm 0.41) \times 10^{-8}$ unit. The corresponding mean value in the neutrophil extracts ($1.3 \pm 0.42 \times 10^{-8}$ unit) is within the range of values found in the present single-cell analysis, implying the results are reliable. A typical voltammogram of a single APL cell after subtracting the blank is shown in Figure 6, curve 7. The PO activity in 14 individual APL cells was determined (see Supporting Information). The PO activities were in the range from 0.93 to 3.1×10^{-7} unit with a mean PO activity of $(2.1 \pm 0.60) \times 10^{-7}$ unit. The corresponding mean value in the APL cell extracts ($2.3 \pm 0.54 \times 10^{-7}$ unit) is within the range of values found in the present single-cell analysis.

CONCLUSION

The voltammetry using a microcell coupled with a dual electrode consisting of a $10\text{-}\mu\text{m}$ -radius Au disk working electrode and a $\sim 80\text{-}\mu\text{m}$ -radius Ag/AgCl reference electrode is capable of analyzing enzyme activity in single cells. However, three factors should be considered. First, the evaporation of the solution should be minimized or eliminated during determination. For ≥ 20 nL of solution, the problem can be easily overcome by positioning the microcell in a constant-humidity chamber. Second, the concentration of the detected analyte of interest in the detected solution should be high enough so that the electrochemical signal can be detected by the micrometer-sized working electrode. The concentration can be achieved through the enzyme-catalyzed reaction by increasing the reaction time and decreasing the detected solution volume. Finally, the concentrations of the biological macromolecules from a single cell in the detected solution should be low enough so that these macromolecules do not interfere with the determination of the analyte of interest. This requires the detected solution volume to be large enough. An additional problem is oxygen reduction in the solution, when an electrochemical reduction reaction of the product of the enzyme-catalyzed reaction is used to determine enzyme activity. A simple method is subtraction of the reduction current of oxygen by recording the blank voltammogram. The technique described here for determining PO in single neutrophils can be applied to determine other enzymes in single cells.

ACKNOWLEDGMENT

This project was supported by the National Natural Science Foundation of China (20235010, 20475033) and the State Key Laboratory of Electroanalytical Chemistry, Changchun, Institute of Applied Chemistry, Chinese Academy of Science. We are grateful to Professor Yuanhua Shao of Peking University for fabricating the dual pipets from θ tubing.

SUPPORTING INFORMATION AVAILABLE

Additional information as noted in text. This material is available free of charge via the Internet at <http://pubs.acs.org>.

Received for review July 1, 2005. Accepted November 1, 2005.

AC051178C